

Supplement of *Clim. Past*, 14, 601–608, 2018
<https://doi.org/10.5194/cp-14-601-2018-supplement>
© Author(s) 2018. This work is distributed under
the Creative Commons Attribution 4.0 License.



Supplement of

Particle shape accounts for instrumental discrepancy in ice core dust size distributions

Marius Folden Simonsen et al.

Correspondence to: Marius Folden Simonsen (msimonse@fys.ku.dk)

The copyright of individual parts of the supplement might differ from the CC BY 4.0 License.

A Bags measured by the Coulter Counter

A.1 Holocene

Bag	Top	Bottom	Top age	Bottom age
Bag	depth (m)	depth (m)	(years b2k)	(years b2k)
300	164.45	165.00	356	358
304	166.65	167.20	363	365
305	167.20	167.75	365	367
321	176.00	176.55	395	397
335	183.70	184.25	423	425
714	392.15	392.70	1980	1989
716	393.25	393.80	1998	2006
746	409.75	410.30	2282	2293
747	410.30	410.85	2293	2303
755	414.70	415.25	2379	2390
759	416.90	417.45	2423	2434
760	417.45	418.00	2434	2446
762	418.55	419.10	2457	2469
788	432.85	433.40	2785	2799
795	436.70	437.25	2884	2899
797	437.80	438.35	2914	2928
799	438.90	439.45	2943	2958
800	439.45	440.00	2958	2974
836	459.25	459.80	3588	3608
837	459.80	460.35	3608	3629
838	460.35	460.90	3629	3650
840	461.45	462.00	3671	3692
842	462.55	463.10	3713	3734
847	465.30	465.85	3822	3845
848	465.85	466.40	3845	3868
850	466.95	467.50	3890	3914
851	467.50	468.05	3914	3937
852	468.05	468.60	3937	3961
854	469.15	469.70	3984	4008

A.2 Glacial

Bag	Top	Bottom	Top age	Bottom age
Bag	depth (m)	depth (m)	(years b2k)	(years b2k)
972	534.05	534.60	17760	21170
973	534.60	535.15	21170	24745
974	535.15	535.70	24745	28783
975	535.70	536.25	28783	33885

B Coincidence

There is no indication of coincidence in the Abakus. If two small particles coincide in the Abakus detector, their combined shadow will make them look like a larger particle. This effect might skew the Abakus distribution towards showing

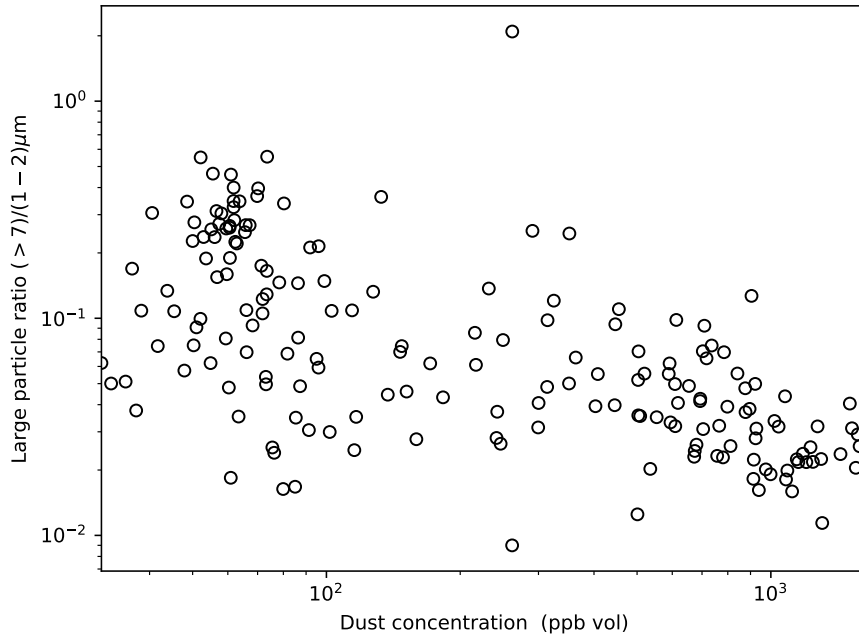


Figure A: The ratio between small and large particle concentration by volume as a function of total dust concentration. The points are 10 cm sections from 533-554 m depth.

more large particles. It has previously been shown that the coincidence effect is negligible for concentrations below 240,000 particles/mL (Saey, 1998). The highest dust concentrations measured in the RECAP core were around 220,000 particles/mL. We will therefore test whether there is a coincidence bias in the following way. If the concentration of small particles is C , the concentration of coincidences is proportional to C^2 . In an ice core dust sample, we would expect the ratio between small and large particles to be more or less independent of the concentration. We can therefore check for coincidence by comparing the ratio between small and large particle concentrations for different total dust concentration. In the glacial, for dust concentrations over 200 ppb, there is no correlation between the relative large particle concentration and the total concentration (figure A). For concentrations smaller than 200, the relative large particle concentration is slightly larger. This could be a climatic signal. We find no significant trend with respect to concentration, suggesting no significant coincidence effect for our measured ice core samples.

C Polystyrene sphere standards

The polystyrene sphere standards were produced by BS-Partikel GmbH, Wiesbaden, Germany. d_{true} is the certified diameter given by the manufacturer, d_{meas} is the diameter measured by the Abakus, and σ_{true} and σ_{meas} are their uncertainties.

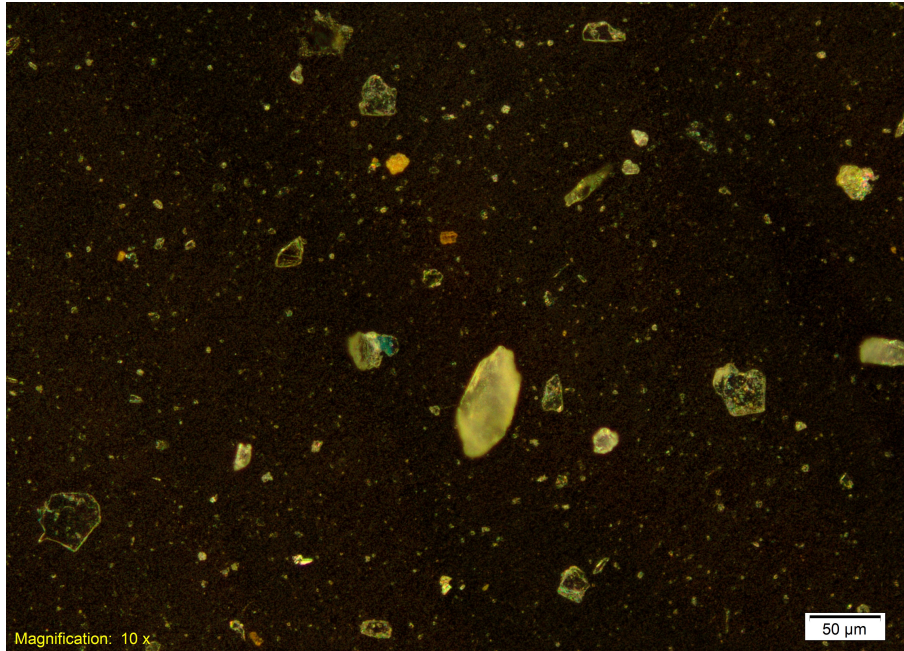


Figure B: Microscope photograph of RECAP Holocene dust from bag 837.

Nominal diameter (μm)	d_{true} (μm)	d_{meas} (μm)	σ_{true} (μm)	σ_{meas} (μm)	Lot No.	Catalog No.
1.5	1.45	1.08	0.04	0.05	LS0248.161	LS0150-05
2	1.97	2.06	0.06	0.05	LS239.111	LS0200-05
4	3.77	3.12	0.14	0.27	LS237.161	LS0400-05
5	4.92	4.96	0.06	0.35	LS122.111	LS0500-05
10	10.37	10.83	0.14	0.71	LS108.509	LS1000-05

D Microscope photographs

Photographs of both glacial and Holocene dust were taken through a microscope (Figures B and C). The highly non-spherical shape is clearly seen. As the particles orient themselves with as low center of mass as possible on the substrate, they will typically lie on their flattest side. The aspect ratio is therefore not directly visible.

E Abakus calibration scheme

The Abakus has to be calibrated in two steps: first to yield the extinction cross section (Section 3.2), and then to account for an aspect ratio different from 1 (Section 3.5). Here is a step-by-step guide to the calibration.

1. Extinction calibration
 - (a) Measure standard polystyrene spheres with the Abakus, preferably at least 5 different sizes. For polar ice, the range 1-20 μm is appropriate.

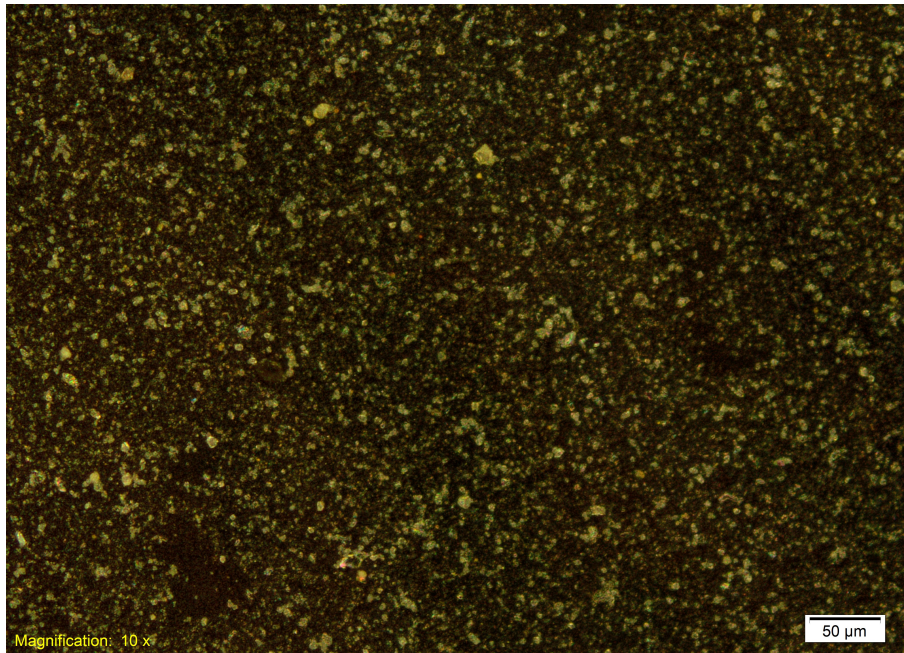


Figure C: Microscope photograph of RECAP glacial dust from bag 975.

- (b) The spheres have a true diameter given by the manufacturer and now also a measured diameter given by the Abakus. The theoretical extinction diameter as a function of true diameter is shown in Figure 2. Divide the measured data by the theoretical curve to get a ratio for each data point.
- (c) Connect each ratio by interpolation or preferably by fitting a smooth function to the ratio versus the measured diameter. This gives a continuous ratio function.
- (d) Multiply the Abakus bin boundaries by the ratio function. The Abakus data with the new bin boundaries are now a histogram of extinction diameters.

2. Aspect ratio calibration

- (a) If the aspect ratio is known, for example from SPES, multiply the Abakus bin boundaries by the cubic root of the aspect ratio. The Abakus data is now calibrated.
- (b) If the aspect ratio is not known, use Coulter Counter data to calibrate the Abakus by the following optimisation algorithm. Multiply the Abakus bin boundaries by a variable c to get nominally calibrated Abakus data.
- (c) Take the logarithm of both Coulter Counter and Abakus data, subtract the two and take the absolute value. The sum of the absolute values is the badness of the optimisation.

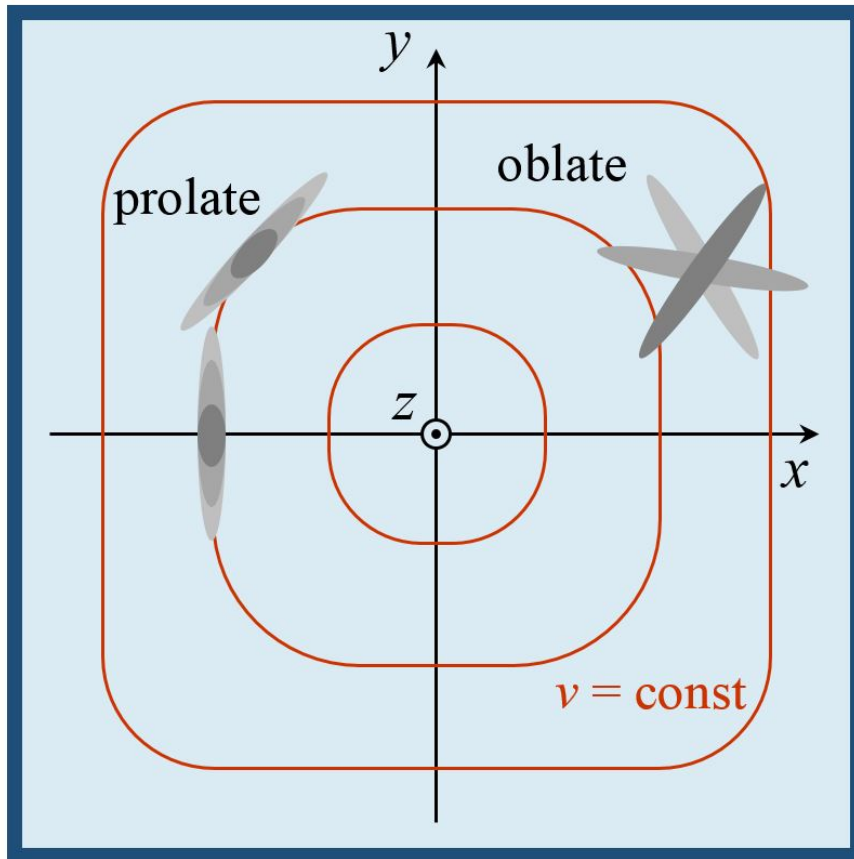


Figure D: The Abakus flow cell. The flow is in the z direction and the laser beam is in the x direction. The red curves are contours of constant flow velocity. Oblate particles are free to rotate in the x, y plane, while prolates can rotate in a plane of constant flow.

- (d) Vary c to minimise badness. The nominally calibrated Abakus data corresponding to minimal badness may be used as calibrated Abakus data.

F Prolate particles

The RECAP samples consist primarily of oblate particles, so the analysis of sections 3.3 and 3.4 have not included prolate particles. The extension to prolate particles is however straight forward, and we show it here for possible future samples dominated by prolates. The aspect ratio of the RECAP samples will now be derived by comparing real Abakus data and modelled Abakus data derived from Coulter Counter data under the assumption that the particles are prolate. Prolate particles are free to rotate in a plane of constant velocity, but cannot rotate out of the plane (Jeffery, 1922). To describe their orientation,

define a cartesian coordinate system with z in the flow direction, x in the laser light direction, and origin at the center of the rectangle (Figure D). If a prolate particle is located at $y = 0$ and $x \neq 0$, its long side will always face the light beam, since its rotation is in the plane orthogonal to the light beam. In the 2D rectangle model (Figure G), this corresponds to the side a always facing the light. This gives a unique d_{ext} for each d_{vol} , and Equation 1 is replaced by

$$\frac{dP(d_{\text{ext}}|d_{\text{vol}})}{d \ln d_{\text{ext}}} = \delta(\ln d_{\text{ext}} - \ln(\alpha d_{\text{vol}})), \quad (\text{A})$$

where δ is the Dirac delta function and

$$\alpha = \sqrt{\frac{\pi}{4c}}. \quad (\text{B})$$

This value of α is calculated by letting c be the aspect ratio of the rectangle, d_{ext} the long side and d_{vol} the diameter of a circle with the same radius as the rectangle. In effect, Equation D means that the distribution of d_{ext} is equal to the distribution of d_{vol} , just with $d_{\text{ext}} = \alpha d_{\text{vol}}$. If a prolate particle is located at $x = 0$ and $y \neq 0$, all rotation angles relative to the light are equally likely. It can therefore be modelled like the oblates. We assume that all positions in the x, y plane are equally likely. For $x \neq 0$ and $y \neq 0$, $\frac{dP(d_{\text{ext}}|d_{\text{vol}})}{d \ln d_{\text{ext}}}$ is a combination of Equation 1 and D. The combination of the equations depend on x and y in a non-trivial manner. However, we assume that the aspect ratio derived from the combination will lie between the aspect ratios derived from Equation 1 and D. To approximate the exact combination, we take the mean of the two distributions. Using Equation 3, modelled Abakus data can be generated from the Coulter Counter data, similar to what we did for the oblate particles. The best correspondence between modelled and real Abakus data is for $c = 0.34 \pm 0.04$ for the glacial and $c = 0.43 \pm 0.08$ for the Holocene. As the correct relative weight of Equation 1 and D in $\frac{dP(d_{\text{ext}}|d_{\text{vol}})}{d \ln d_{\text{ext}}}$ is uncertain, an upper bound on the aspect ratio can be calculated by using only Equation D. This gives $c = 0.37 \pm 0.03$ for the glacial and $c = 0.45 \pm 0.06$ for the Holocene. The uncertainty on c arising from a wrong relative weight of Equation 1 and D is therefore smaller than the uncertainty from other sources, and can be neglected. In conclusion, the aspect ratio derived from comparing Abakus to Coulter Counter data is less extreme when prolate rather than oblate particles are assumed.

ADDA simulations of prolate particles can also be used to extract an aspect ratio from the SPES data. This is rather artificial, as the SPES data shows that the particles are oblate. However, we do it to show that adding a fraction of prolates does not change the fitted aspect ratio significantly. As described in section 3.3, the mean optical thickness ρ is calculated as function of extinction cross section σ_{ext} for different aspect ratios c (Figure E). These curves are interpolated to generate a contour plot of c in $\rho, \sigma_{\text{ext}}$ space. The mean ρ curve is then calculated for the aspect ratios 0.25, 0.33 and 0.50 for prolate particles. By fitting these mean ρ curves to the oblate aspect ratio contour, it is found that they correspond to oblate particles of aspect ratio 0.23, 0.28 and 0.41 respectively. The fit is only performed for σ_{ext} values between the 0.25 and 0.75 quantiles of the SPES data, ie. between the blue lines of Figure 6. By interpolating between the prolate/oblate aspect ratio pairs, it is found that the prolate aspect ratios corresponding to the oblate aspect ratios of 0.33 and 0.39 of

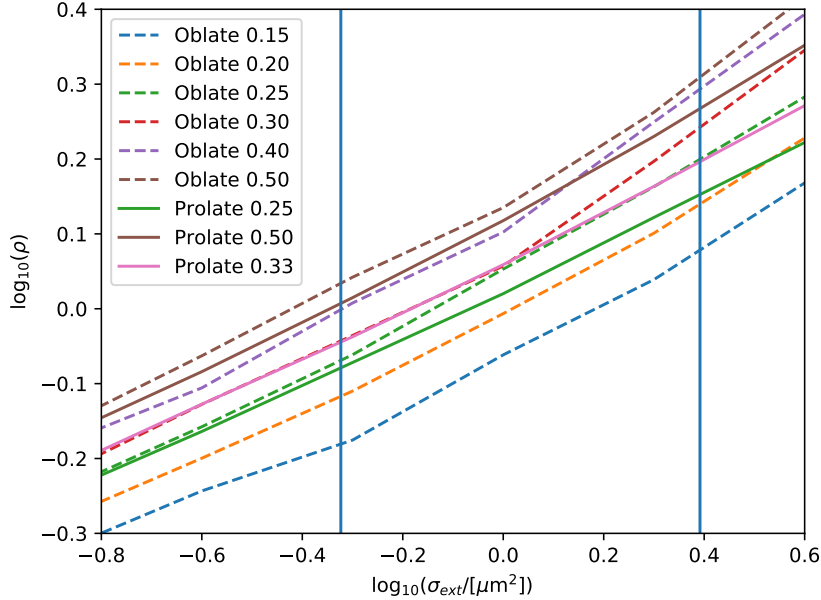


Figure E: Mean optical thickness curves for oblate and prolate particles for different aspect ratios indicated in the legend.

the RECAP glacial and Holocene samples are 0.39 and 0.47 respectively (Figure F). The ADDA simulations therefore predict less extreme aspect ratios for prolates than for oblates, similarly to the Abakus/Coulter Counter comparison. This analysis is however artificial in the sense that the RECAP samples are dominated by oblates and not prolates.

G Extinction diameter calculation in the 2D model

The particles in the Abakus are modelled as 2D rectangles, for which all rotation angles are equally likely (Figure G). The cross section of the particle is equal to d_{ext} in the 2D model.

G.1 Rod

For calculating the cross section of a rectangle, the cross section of a rod is needed. We define a rod with length l and zero width. For an angle of rotation ϕ , the cross section is $d_{\text{ext}} = l \sin \phi$. From symmetry, the ϕ values are confined to $\phi \in [0, \frac{\pi}{2}]$. Assuming a uniform probability distribution for the angle, the probability of measuring the particle in the interval $[\phi, \phi + d\phi]$ is $dP(\phi; d\phi) = \frac{2}{\pi} d\phi$, which is normally written $\frac{dP(\phi)}{d\phi} = \frac{2}{\pi}$.

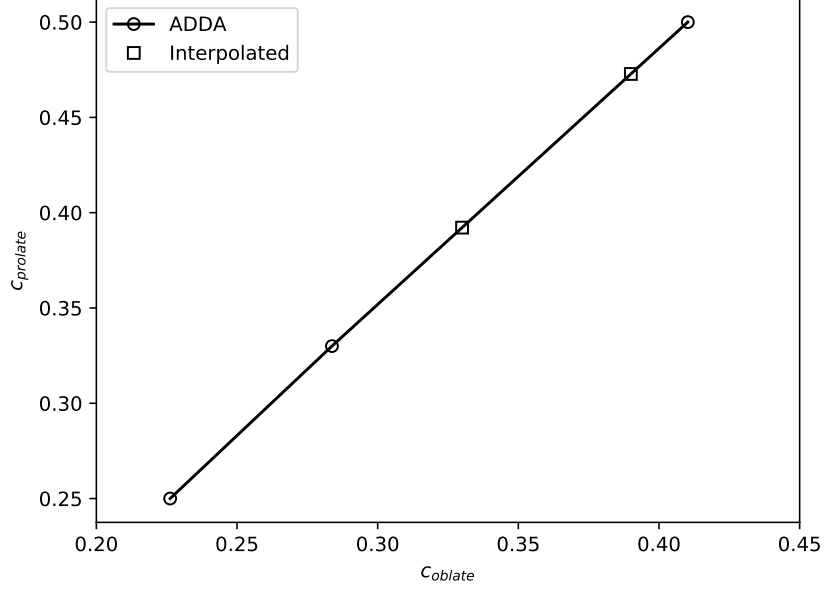


Figure F: ADDA simulated prolate aspect ratios for the corresponding oblate aspect ratios, derived from Figure E. The squares are at c_{oblate} values of 0.33 and 0.39, interpolated between the simulated values.

For converting this to d_{ext} space, $d\phi$ needs to be expressed in terms of dd_{ext} :

$$d_{\text{ext}} = l \sin \phi \quad (\text{C})$$

$$\Rightarrow dd_{\text{ext}} = l \cos \phi d\phi \quad (\text{D})$$

$$\Rightarrow d\phi = \frac{1}{\sqrt{l^2 - d_{\text{ext}}^2}} dd_{\text{ext}} \quad (\text{E})$$

Therefore

$$\frac{dP(d_{\text{ext}})}{dd_{\text{ext}}} = \frac{2}{\pi} \frac{1}{\sqrt{l^2 - d_{\text{ext}}^2}} \quad (\text{F})$$

$$\Rightarrow \frac{dP(d_{\text{ext}})}{d \ln d_{\text{ext}}} = z, \quad (\text{G})$$

where

$$z = \frac{2}{\pi} \frac{1}{\sqrt{\left(\frac{l}{d_{\text{ext}}}\right)^2 - 1}}. \quad (\text{H})$$

It is seen that it diverges for $d_{\text{ext}} \rightarrow l$, because d_{ext} is almost constant as a function of angle when the rod is close to being perpendicular to the light source.

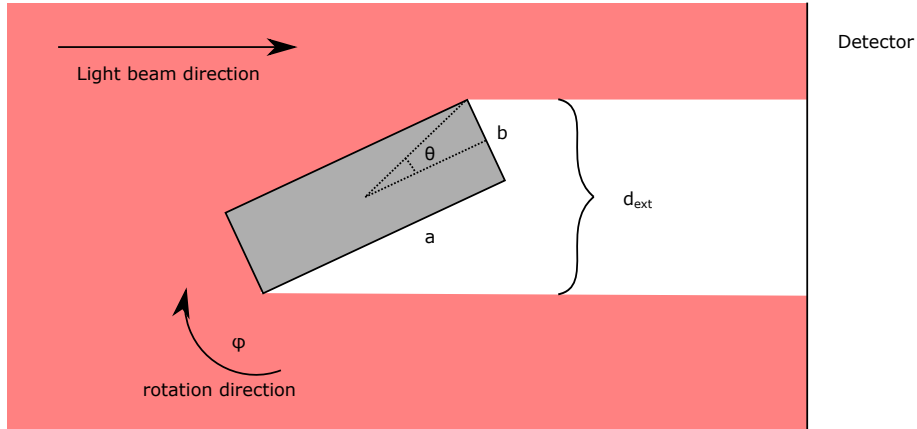


Figure G: 2D model of the particle orientation in the Abakus.

G.2 Rectangle

Consider a rectangle with side lengths a and b . As for the rod, by symmetry, it is only necessary to consider the angles $\phi \in [0, \frac{\pi}{2}]$. In this case the cross section is given by the cross section of the diagonal. This is just the cross section of a rod rotated by

$$\phi_+ = \phi + \theta \quad (\text{I})$$

$$\Rightarrow \phi_+ \in [\theta, \frac{\pi}{2} + \theta], \quad (\text{J})$$

where θ is the angle between the side a and the diagonal. If ϕ is uniformly distributed in $[0, \frac{\pi}{2}]$, so is ϕ_+ in $[\theta, \frac{\pi}{2} + \theta]$. The derivation for the rod is only valid when d_{ext} is a monotonous function of ϕ . This means that it can only be directly applied for $\phi_+ < \frac{\pi}{2}$. However, due to symmetry, the cross section is the same for $\phi_+ = \frac{\pi}{2} + \Delta\phi$ and $\phi_+ = \frac{\pi}{2} - \Delta\phi$, for any $\Delta\phi$. Therefore, the probability of measuring a cross section corresponding to $\phi \in [\frac{\pi}{2} - \theta, \frac{\pi}{2}]$ is twice as high as the probability of measuring the cross section of a rod in this interval. The cross section of $\frac{\pi}{2} - \theta$ is a . This means that the probability distribution is

$$\frac{dP(d_{\text{ext}})}{d \ln d_{\text{ext}}} = \begin{cases} 0 & \text{for } d_{\text{ext}} < b \\ z & \text{for } b < d_{\text{ext}} < a \\ 2z & \text{for } a < d_{\text{ext}} < \sqrt{a^2 + b^2} \end{cases}, \quad (\text{K})$$

for

$$z = \frac{2}{\pi} \frac{1}{\sqrt{\frac{a^2 + b^2}{d_{\text{ext}}^2} - 1}}. \quad (\text{L})$$

H Replicate ice core measurements

The upper 93 m of the RECAP ice core has been measured twice (Figure H). This means that two parallel sticks have been cut from the core, each of which

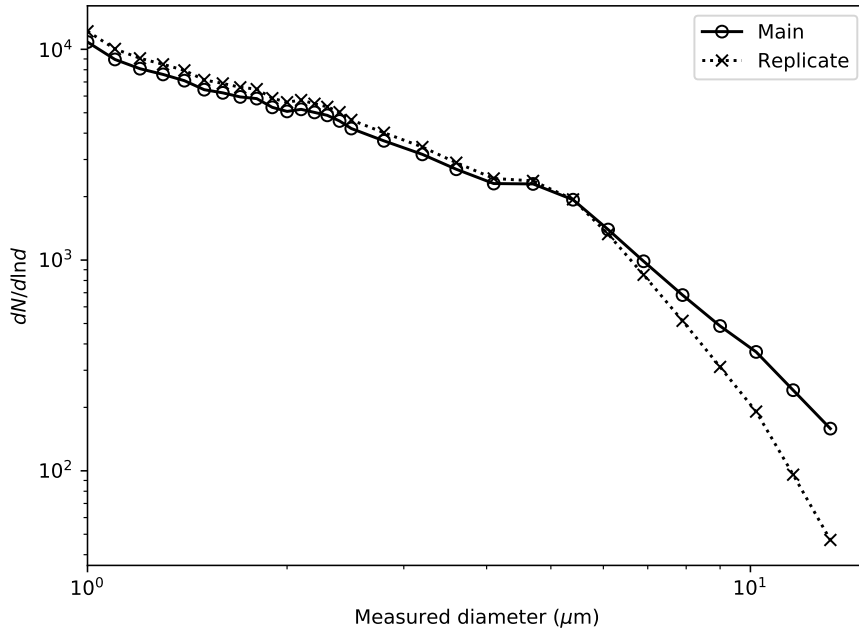


Figure H: The upper 93 m of the RECAP ice core measured twice with the Abakus.

has been measured on the Copenhagen CFA system. The CFA system was modified slightly between the two measurement campaigns, including changes in the pump and tubing setup, as well as general wear and roughening of the tubing walls. Therefore, the difference between the two measurements most likely reflects the error introduced by the CFA system. For the smaller particles, the replicate values are 12 % larger than the main. In comparison, for the large particles the replicate measurement has up to 3 times lower values than the main measurement. This is probably because the transport of the large particles from the melt head to the instrument depends more on the specific system setup than the small particle transport.

The difference between the two measurements is used as uncertainty for the Abakus measurements. However, a minimum uncertainty of 12 % is used, since the crossing of the two curves gives an artificially low difference.

I Detection limit

The number size distribution is a decreasing function even for the smallest detectable diameters (Figure I). This means that there are most likely many more particles below the detection limit than above. The total counts therefore depends heavily on where the lower cutoff is. After calibration, the Coulter Counter and the calibrated Abakus give almost the same total number of particles for the same size range.

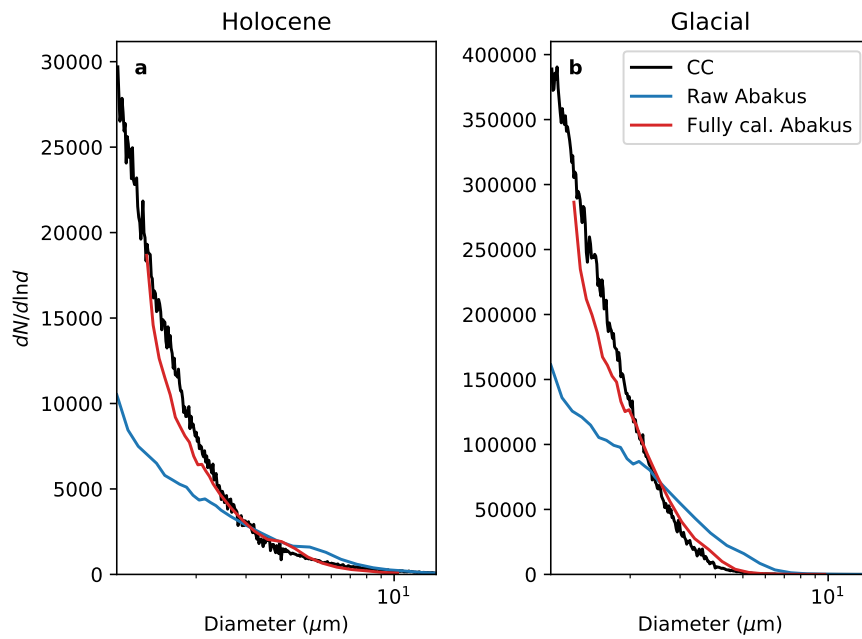


Figure I: Figure 5a,b on a linear vertical scale.

References

- Jeffery, G. B.: The motion of ellipsoidal particles immersed in a viscous fluid, in: Proceedings of the royal society of London A: Mathematical, physical and engineering sciences, 715, pp. 161–179, The Royal Society, 1922.
- Saey, P.: Diplomarbeit im Studiengang Physik, Master's thesis, Fakultät für Physik und Astronomie, Ruprecht-Karls-Universität Heidelberg, 1998.